

Analysing Raman Maps of Graphene using Wolfram Mathematica

BY

DÓNAL FLANAGAN

The following is a companion guide to a Mathematica computer programme written by Dónal Flanagan as part of a M.Sc. thesis in physics at the Freie Universität Berlin.

The work presented in this document was carried out in the research group of Prof. Dr. Stephanie Reich (FU Berlin) as part of a collaborative research project on surface enhanced Raman spectroscopy with Atotech Berlin GmbH and the group of Prof. Dr. Eric Anglaret of Université Montpellier II.

The programme is designed for the analysis of CVD graphene but may be easily altered to analyse maps of exfoliated graphene and other materials such as dyes, etc.

Contents

1	Aim of the Programme	1
2	Introduction to the Programme	2
2.1	Layout of the programme	2
2.2	Saving data in the correct format.....	3
2.3	Importing data.....	3
2.4	Exporting data.....	3
2.5	Using the programme.....	4
3	The Raman Spectrum of Graphene	5
3.1	Peaks.....	5
3.2	Number of layers.....	7
3.3	Strain	8
4	Data Analysis	10
4.1	Fitting the background	10
4.2	Fitting the single peaks.....	10
4.3	Fitting peaks using constraints.....	11
4.4	Fitting overlapping peaks	12
4.5	Removing multilayer graphene	13
4.6	Creating map images and histograms	14
4.6.1	Complete list of images generated.....	15
5	Additional Programmes	19
5.1	Map, histogram plotting programme	19
5.2	Normalization programme	20
5.3	Single plot checker	20
5.4	PolynomialFit.m	20
6	Bibliography	21

Aim of the Programme

SERS is a phenomenon in which the intensity of the Raman signal is increased by localized surface plasmon resonances (LSPR) occurring in noble metal nanostructures (electromagnetic enhancement)[2][3] or by a resonant charge transfer effect (chemical enhancement)[4].

Graphene is a one atom thick, two-dimensional crystal of carbon atoms with a hexagonal lattice structure. It has a wealth of truly unusual properties due to its unique electronic band structure. Graphene is extremely strong, flexible, and highly conductive both electrically and thermally. It has a negative thermal expansion coefficient[5] and has been shown to exhibit the quantum Hall effect[6][7].

There are numerous reasons for which it is an ideal analyte for studying SERS [8][9]:

- It has a uniform thickness of one atom which provides a homogenous covering. This increases the probability of detecting a SERS hotspot while reducing the probability of detecting a pseudo-enhanced signal due to analyte accumulating at one spot.
- It is 98% transparent, allowing the laser light to pass through the analyte and strike the nanostructures, exciting the LSPRs.
- It has a strong Raman signal due to its electronic band structure.
- It is chemically stable and passivates the graphene against oxidation[10][11] (at timescales below five months in ambient conditions [12]).
- It has a very informative Raman spectrum which allows many conclusions to be drawn about the state of the surface [13].

Quantification of the enhancement effect requires analysis of the intensity of the Raman signal with respect to the surface topology.

Due to the fact that the Raman spectrum of graphene can change quite drastically due to enhancement, strain, defects, and multiple layers, commercial graphing software such as Origin is often inadequate for analysing large numbers of spectra.

Introduction to the Programme

2.1 Layout of the programme

The programme is divided into three sections, each described below. Each of these sections must be initialized, one after the other, by placing the text cursor within the section/code and pressing *Shift+Enter*.

Functions library: This contains small programmes, called *functions*, which carry out specific tasks using given parameters. Each function is *called* multiple times by the main programme.

For example; we use a function to import the data files. The function is called each time we need to import a data file. The name of the file to be imported is the parameter which must be specified. The function contains the code that imports a file but the name of the file will be different each time as the main programme analyses each spectrum in the Raman map/data set.

Main programme

Import data: This section of the programme is used to select the data set to be analysed.

Fitting programme: The third section is the main programme. The data files are imported and distributed to each kernel of the computer (two in a dualcore, four in a quadcore, etc.). Each kernel runs the programme separately (in parallel) to increase time-efficiency. The peaks are fit and each spectrum is exported along with a file containing the fitted data values. Finally, 2D and 3D images of the relevant results are created and exported.

The main programme is commented with sections (1, 2, 3...) and subsections (1.1, 1.2, 1.3...). These labels refer to the function, in the functions library, being used in said subsection. If you are unsure what is happening at a certain point in the programme, the answer can be deduced by searching out the relevant function in the functions library and examining it with the parameters being used.

Remember, Mathematica has a very complete help section which will help explain any unfamiliar terms in the Wolfram language.

2.2 Saving data in the correct format

The individual data files in the Raman map should be labelled according to their {x,y} coordinate in the format "mapname_x_y".

For example, when using the Labspec programme from an Xplora Raman spectrometer, after recording the Raman map, click on the window in which all of the spectra are displayed. Click on *File -> Split* and type a *mapname*. The individual spectra of the map are then exported as *mapname_x_y*.

Function 8.1, *importdata*, in the functions library is currently set to import TSV (tab-separated variable) .txt files. If your files are in a different format simply replace the relevant parts in the function, e.g. .txt -> .dat, TSV -> CSV, etc.

2.3 Importing data

The data files containing the individual spectra are imported one by one and distributed to each kernel of the computer. The programme automatically starts importing at file {x,y}={0,0} and continues until it reaches the file selected by the user. To analyse a complete dataset simply select the last file.

2.4 Exporting data

The image of each spectrum, and it's corresponding fit-parameters results file, are all exported separately. This is in case the programme crashes. This rarely happens but for very large maps, which can take hours to process, it is better to have the individual results, just in case. The images of the fitted spectra are automatically exported to a folder named "*mapname;Spectra*".

The fit parameters for the individual spectra are exported as separate .txt files, along with a single .txt file containing the complete set of results, to a folder named "*mapname;Results*".

Finally, various 2D and 3D images of the complete Raman map are exported to a folder named "*mapname;Fitted Maps*". These are described in greater detail in the Data Analysis section.

All of these results folders are created in the parent folder of the Raman data set being analysed.

2.5 Using the programme

Step 1: Initialize the functions

Place the text cursor in the 'Functions' section and press *Shift+Enter*.

Step 2: Select the data

Place the text cursor in the Import Data section and press *Shift+Enter*.

Ensure that the filepath of the *PolynomialFit.m* function is correct.

Click the '*Browse...*' button, navigate to the datasets you wish to fit, and select the last spectrum you wish to analyse.

Step 3: Set the variables and execute the programme

Set the variables to appropriate values:

m: The normalization constant for the distance vs number of plots for the 2D and 3D maps, i.e. if the step size between measurements is 0.5 micrometres then set *m*=0.5 to normalize the distance for the axes of the 2D and 3D map images.

bin: The size of the steps in the histograms.

polydeg: The order of the polynomial which will be fit to the background. A higher number works better if your background tends to change drastically, or is uneven, due to inter-band transitions, etc.

distdatamax: At the end of the programme, after fitting all of the spectra we will create a histogram of the G peak areas to identify the average value. We cannot take the complete data set when calculating this average because (for SERS samples) there could be highly enhanced areas which should not contribute to the average value. We specify *distdatamax* as the maximum value below which we accept G peak areas as contributing to the average. i.e. unenhanced areas or areas indicative of an average enhancement across the sample.

(*distdatamax* and *bin* are generally just guesses initially and the histograms may be incorrect. In this case, rather than fitting all of the spectra again, just use the "map, histogram plotting programme" to import the results array and replot the maps and histograms with better parameters.)

Press *Shift+Enter*.

The Raman Spectrum of Graphene

The following is a very short introduction to the Raman spectrum of graphene. Please see the sources cited in the bibliography section for a more in-depth explanation.

3.1 Peaks

The Raman spectrum of graphene is dominated by the G and 2D bands. The G band (the graphitic line), which appears in the Raman spectrum at $\sim 1582\text{cm}^{-1}$, is due to a degenerate optical phonon mode with E_{2g} symmetry at the Brillouin zone centre Γ . Of the six normal modes of graphene at $\mathbf{q} = 0$, only the two which make up the G mode are Raman active and degenerate [14].

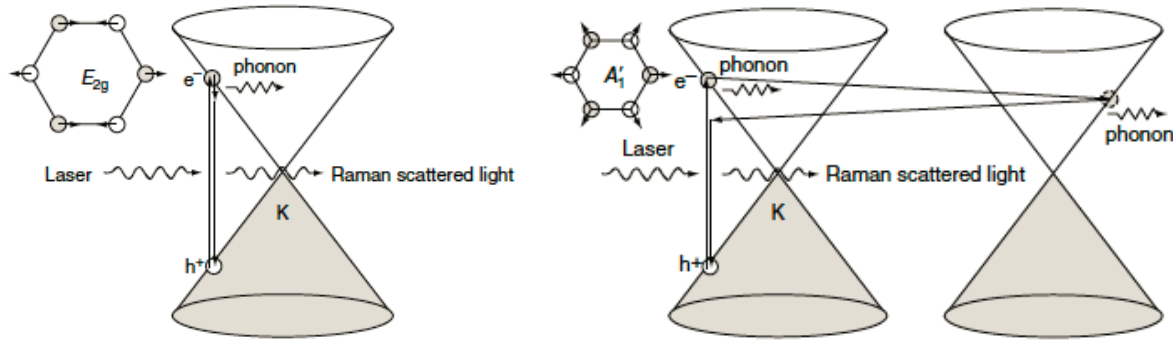


Fig. 1: (Left) The G band Raman scattering process and the vibration of the E_{2g} phonon mode. (Right) The double resonant 2D band scattering process and the corresponding vibration of the A'_1 phonon mode [15].

The 2D band (also called G' and D*) is an overtone of the D band appearing in the range $2600 - 2800\text{cm}^{-1}$, which requires a two-phonon scattering process near the K point involving A'_1 phonons. To explain the 2D band scattering it is best to first define the scattering process of the D mode, another important feature of the graphene spectrum.

The D band is a defect induced band in the range $1300 - 1400\text{cm}^{-1}$. The D mode arises from a double resonant Raman scattering process first put forward by Reich and Thomsen [16]. This double resonance is a fourth order perturbation theory process

3 The Raman Spectrum of Graphene

which explains the dependence of the energy of the D mode in Raman spectra on the wavelength of the exciting laser line. It also explains the strong intensity of the D band and its overtone, the 2D band.

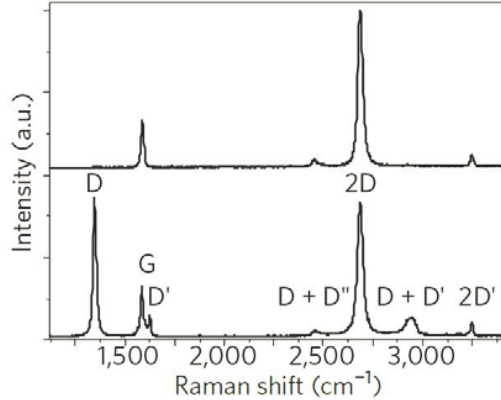


Fig. 2: The Raman spectrum of high quality (top) and defective (bottom) monolayer graphene. The D peak only occurs in the presence of defects. [17]

Fig. 3 shows the Raman scattering process of the D peak between two neighbouring Dirac points. First, an electron-hole pair is excited to the conduction band (near the K point) by an incident photon of energy E_L . A phonon-electron scattering occurs, producing a phonon of energy (D) and wavevector (D) , which scatters the electron to the second band (at the K' point). The electron is then elastically scattered by lattice defects and finally, the electron-hole pair recombine, conserving \mathbf{k} .

This scattering process does not occur in defect-free graphene/graphite because zone-boundary phonons do not satisfy the fundamental Raman selection rule $\mathbf{q} = \mathbf{0}$. The D' band, also shown in Fig. 3, occurs due a similar process involving intra-valley transitions [18].

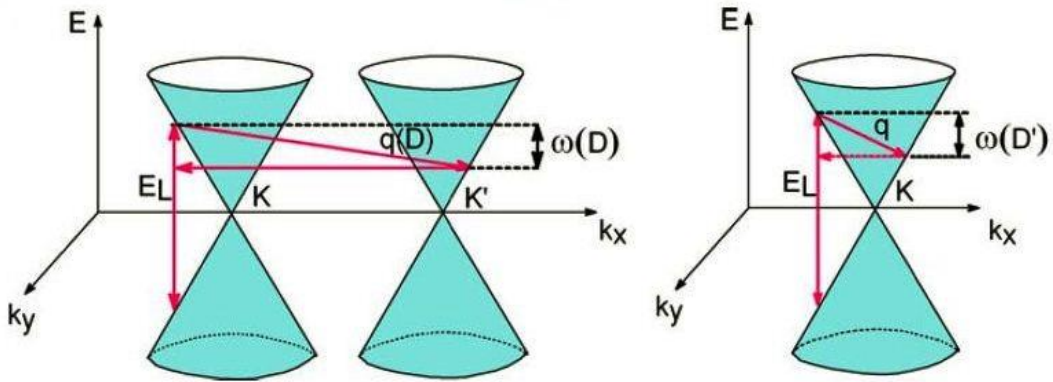


Fig. 3: The D mode (left) and D' mode (right) double resonant scattering processes [15].

The 2D band is an overtone of the D peak where, instead of backscattering off a defect, the electron is scattered by a second phonon. One might expect the 2D transition to be weaker than G as it is a second-order process, but both of the transitions involved are resonant processes so the 2D band is in fact stronger than the G band.

As mentioned previously, the Raman spectrum of graphene contains a lot of information. An examination of the above peaks allows a great deal to be deduced about the state of the graphene layer and its interaction with the surface.

3.2 Number of layers

The intensity of the G peak has been shown to increase with the number of layers up to seven layers, at which point it begins to decrease in intensity [19].

In the case of mechanically exfoliated graphene, multiple layers exhibit the Bernal (AB) stacking structure as this is the structure of graphite, from which the layers have been exfoliated. In the Bernal stacking configuration a B carbon atom of the top layer is positioned above an A carbon atom of the bottom layer and the two are connected by a π -bond [20].

In this case, the line-shape of the 2D band reflects the electronic band structure of the graphene. When a second layer of graphene is added to the first, the two valence electrons in the unit cells form π -bonds between the layers. This causes both the conduction and valence bands to separate into two bands as shown below.

Thus, there are four different possibilities for the 2D double resonance scattering process, each with a slightly different energy. This results in a broadening of the peak, as shown in Fig. 4. As the number of layers increases, the electronic band structure, and therefore the 2D peak, continues to change until it approaches that of graphite in the limit of infinite layers.

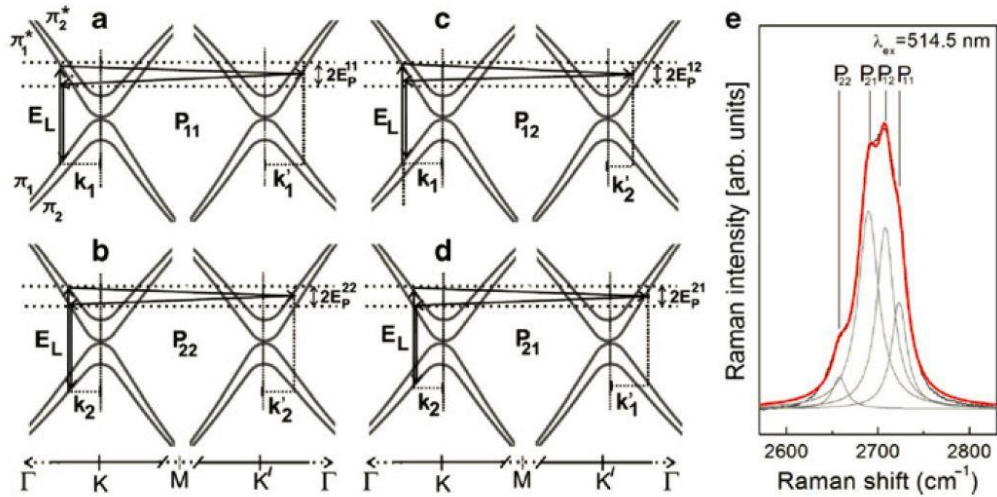


Fig. 4: (Left) The electronic energy band dispersion of bilayer graphene near the K and K' points. (Left) The valence and conduction π -orbitals have separated in two, allowing four different 2D scattering processes. (Right) The resulting broadened 2D peak [21].

3 The Raman Spectrum of Graphene

However, multilayer graphene produced by CVD often exhibits different, non-uniform stacking structures such as Moiré patterns. The interlayer interaction for such a case is weaker than that of AB stacked layers (in which the interaction is already quite weak).

This results in the vibrational and electronic structures, and therefore the Raman signal, of the multiple layers resembling those of a collection of independent, single layers of graphene.

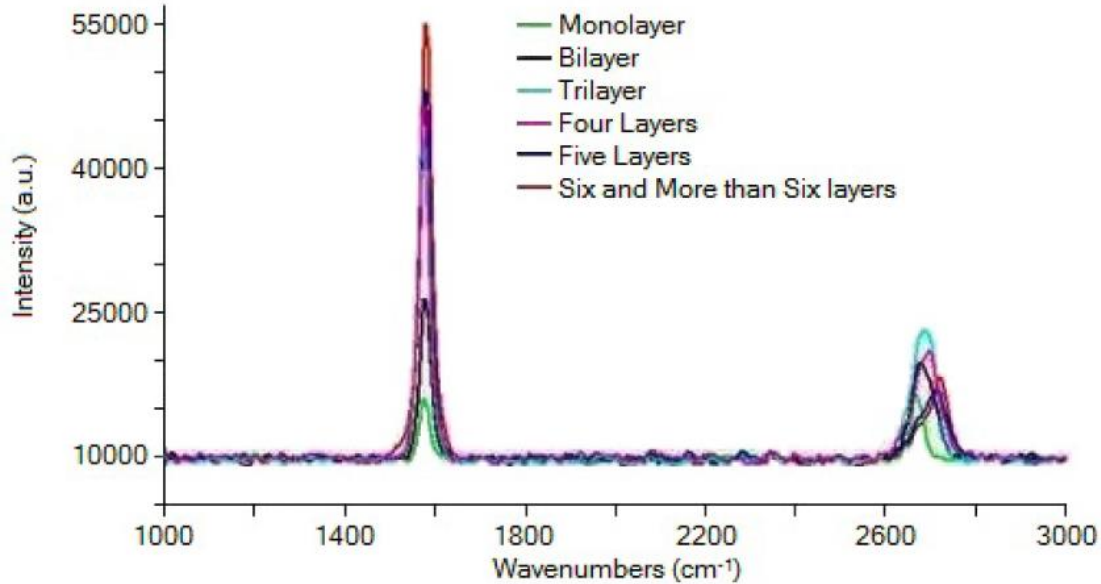


Fig. 5: The I_{2D}/I_G ratio is a reliable indicator of the number of graphene layers [22]

The 2D peak retains its Lorentzian line-shape but increases in intensity due to the increased amount of scattering media. Therefore the line-shape of the 2D peak is not truly indicative of the number of layers when not dealing with mechanically exfoliated graphene [15].

Since the G band increases with the increasing number of layers but then begins to decrease, it alone is also not a truly accurate indication of the number of layers. The 2D peak is a good indicator of mono- vs. multi-layer graphene but not the number of layers, although it does decrease in intensity as the number of layers increases.

Therefore, the ratio of the 2D to G peak is usually used to determine the number of layers of graphene (Fig. 5).

3.3 Strain

The interatomic distance and crystal structure of graphene can be deformed by the application of strain. Strain can be applied as tension or compression and can be

applied uniaxially or biaxially. In general, the application of tensile strain causes redshifting and the compression causes blue-shifting of phonon frequencies [23].

The application of uniaxial strain causes the sub-lattice symmetry to break, which in turn causes the G peak to split into two separate peaks, the G^+ peak and the G^- peak [21]. This splitting is proportional to the applied strain and the splitting can therefore be used to estimate the uniaxial strain.

The 2D peak also splits under strain and exhibits an even more sensitive reaction. This phenomenon has been shown to be the result of a strain induced additional inner double resonance (TO phonon) scattering mechanism and asymmetry of the Brillouin zone [23].

The splitting of the 2D peak under strain also exhibits a dependence on the polarization of the electromagnetic radiation with respect to the strain axis.

Clearly, by careful analysis of the Raman spectra much can be said about the system under analysis. Not only can the quality and amount of analyte be observed, the strain dependence of the 2D peak can also be used in many circumstances to determine how well the graphene is adhering to the nanostructured surface. This is quite beneficial since the light intensity decreases drastically within a few nanometres of the plasmonically resonating nanostructures. If the analyte is not in close contact with the surface, potentially significant enhancement conditions may be overlooked.

The graphene is often stretched across the nanostructures when in close contact with the surface. These small strain areas, being in direct contact with the nanostructures can be significantly enhanced and are both an indicator of enhancement and indicative of good surface-analyte contact across the entire sample.

Data Analysis

4.1 Fitting the background

An n^{th} order polynomial is fit to the background.

The order of the polynomial is assigned the variable name "*polydeg*". *polydeg* is initially set equal to 6 to ensure that the fit is accurate, regardless of changes in the background due to inter-band transitions, excitation wavelength, etc.

To ensure an accurate background fit, regions containing peaks must be excluded from the dataset used to fit the background. Areas to be included in the background fit are defined in function 11.1 *extractbackground*.

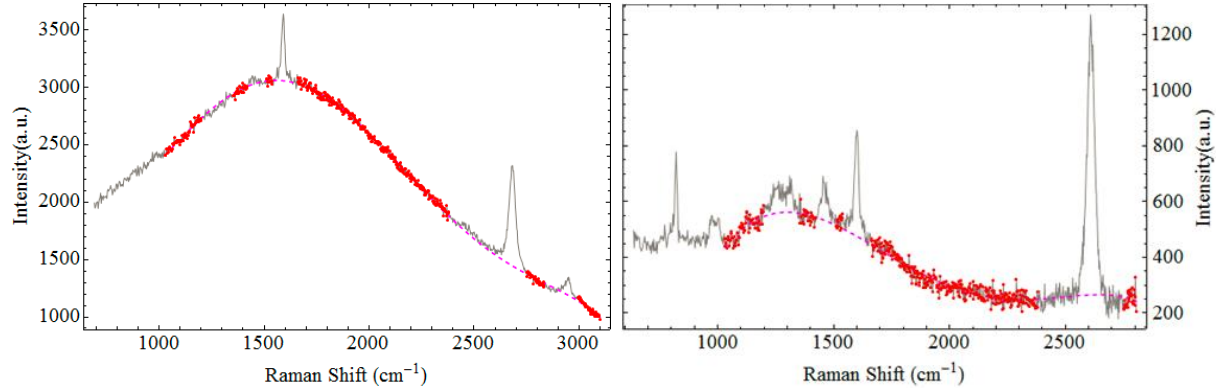


Fig. 6: Examples of a 6th degree polynomial background fit to graphene spectra. The data points used for the fits are shown in red and the fitted background is plotted in pink. (Left) A sample measured at 532nm showing a fluorescent background, G and 2D peaks. (Right) A sample measured at 785nm showing D, G, and 2D peaks as well as PMMA peaks at 816cm⁻¹, 990cm⁻¹ and 1460cm⁻¹.

4.2 Fitting the single peaks

The areas containing the D, G, and 2D peaks are each evaluated separately. The ranges around the peaks are defined in the array *peakrangelist* (func. 10.1). Mathematica does not allow both initial estimates of parameters and parameter constraints to be input to a fitting function, it was found that initial estimates generally produced better results.

The initial estimation of the peak is made by extracting the data surrounding the peak position (func. 10.3) and taking the data points of lowest and highest intensity (func. 12.1). The difference between these points is taken as an initial estimation for the amplitude, the FWHM is assumed to be 20cm^{-1} , and both are used to calculate an initial guess for area. The initial value for the position of the peak is given by the x-value of the data point of highest intensity (y-value). A Lorentzian is then fit to the extracted data set using these initial parameters (func. 14.2).

To prevent bad fits the variance of each fit function from the experimental data is compared with the residuals of the background fit to the experimental data in the same area. If the background fit is found to have a smaller variance, the fitted peak is disregarded and area, amplitude, position and FWHM values of zero are returned (sect. 18).

4.3 Fitting peaks using constraints

The D peak is often not present. It was found that when a peak was not present, but initial parameters were still fed to the fitting function, the result was invariably a non-existent peak fitted to the background data. This quite often resulted in a broad, low-amplitude peak which was barely visible but returned a very large area. To avoid this, constraints can be applied to the fit function (func. 14.1) rather than using initial parameter estimations.

For example, the initial estimate for the area can be used as an upper limit rather than an initial parameter. This has the benefit of preventing an extremely large peak being fit where there is none, but the disadvantage of preventing the programme from accurately fitting very broad D-peaks such as in the case of amorphous carbon. Depending on the sample this may be acceptable however, as the D peaks in such areas are usually large enough to draw attention to the presence of an anomaly on the surface in any case. The coordinates of defective or multilayer areas can be found from the 2D and 3D maps, and the corresponding spectra checked.

A constrained Lorentzian fitting function is present in the functions library (func. 14.1), but is not used in the main programme. After the Mathematica 10 update it became problematic but at that point it was no longer necessary for the programme. The variance comparison function prevented bad fits from being returned. In general, finding the correct limits for parameter constraints can be difficult. Both limits which are too large, and too small, return very bad results. A process of trial and error is necessary to find the appropriate parameters. (Note that constraints are used in functions 14.3 and 14.4 for fitting the strained 2D peaks and work very well.)

4.4 Fitting overlapping peaks

In the presence of strain the 2D peak of graphene splits. Since the strain peak is often of interest but not always present, care must be taken to accurately search for occurrences. To this end, three different models are fit to the data surrounding the 2D peak (2300cm^{-1} to 2800cm^{-1}).

- The first model is a Lorentzian fit to the 2D peak using initial parameter estimates, as described previously (func. 14.2).
- The second model fits a Lorentzian constrained to a position between $2605\text{cm}^{-1} < x_0 < 2660\text{cm}^{-1}$ for the 2D peak, and a Gaussian constrained to $2440\text{cm}^{-1} < x_0 < 2500\text{cm}^{-1}$ for the D+D" peak (func. 14.3).
- The third model is the same as the second but with an additional Lorentzian constrained to $2540\text{cm}^{-1} < x_0 < 2600\text{cm}^{-1}$ to fit the strained 2D peak (func. 14.4).

(Note that the positions of these peaks are dependent on wavelength but the relative values of the constraints should generally remain the same as they have been found to work very well.)

The standard deviation of the experimental data to the three fits is compared and the model with the smallest deviation from the data is taken as the correct fit (sect. 17.2, 17.3, 17.4).

When the peak is not present, or has an unusual shape, a fit function with a negative area can sometimes be returned. This was found to occur quite often when attempting to fit multiple functions to a single peak. If such a function is returned, the standard deviation is automatically set to infinity, guaranteeing that the fit is disregarded and zero values are returned (func 17.1).

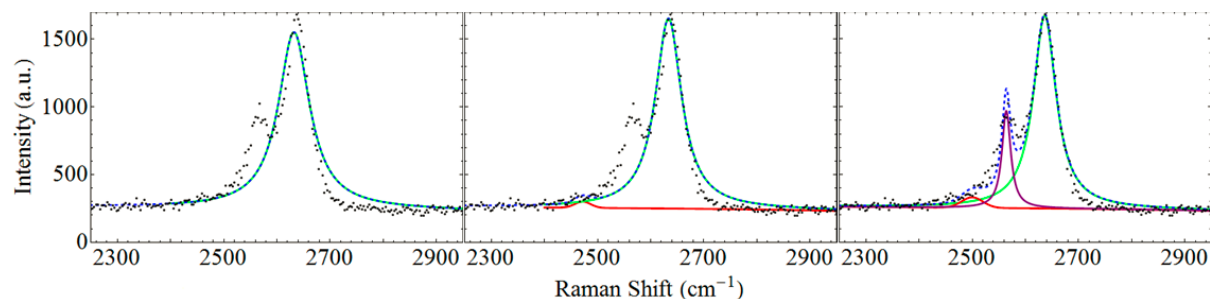


Fig. 7: A spectrum featuring a strained 2D peak. The three fits are shown. The 2D peak in green, the strained 2D peak in purple and the D+D" peak in red. The complete model is shown by the blue dashed line. The third model has the lowest standard deviation and was correctly chosen by the programme as the best fit.

4.5 Removing multilayer graphene

Areas of multilayer graphene cause an increase in the Raman signal intensity due to an excess of analyte. To accurately assess the intensity of the Raman map, one must first remove such falsely enhanced areas. This is also necessary to evaluate the quality of the graphene.

For CVD graphene, multiple layers can be evaluated by the fact that the G-peak intensity is greater than that of the 2D-peak. Therefore, we remove all areas for which the ratio below is true.

$$\frac{I_{2D}}{I_G} < 1$$

The data points are removed from the results array (sect. 27). and, in the 2D and 3D maps, the empty multilayer areas are interpolated over from the surrounding points

It is important to note that for *exfoliated* graphene, due to the Bernal stacking configuration of the graphene sheets, multiple layers result in splitting of the 2D peak rather than a change in the I_{2D}/I_G ratio. This programme is designed to analyse CVD graphene samples. Analysis of multiple layers of exfoliated graphene could be achieved by adapting the overlapping peaks section used to analyse the strained 2D peak.

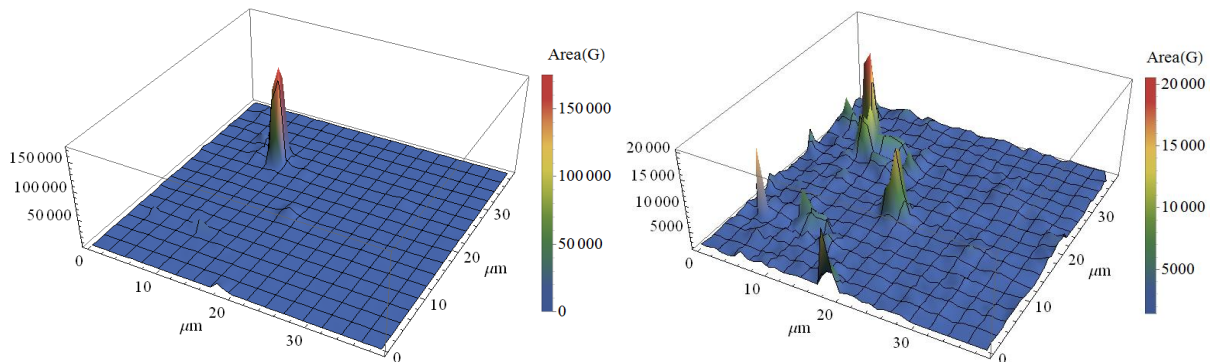


Fig. 8: 3D maps of the area under the G-peak for a sample of graphene on nanostructured Cu before (left) and after (right) removal of the areas containing multiple graphene layers. The false enhancement due to the multiple layers (left) hides the true topography of the Raman signal.

This function can be very useful when producing CVD graphene as it allows the user to check the quality of the graphene, as well as determine the size and dispersion of growth sites. To include multilayer areas in the 2D and 3D maps, simply delete or 'comment out' section 27.

4.6 Creating map images and histograms

A number of 2D and 3D 'maps' of the surface are automatically generated by the programme.

The 2D and 3D map-plotting functions are contained in func. 26.5 and func. 26.6, respectively. The colour scheme, units, scale, etc. can be edited within these functions. The x- and y-axes on both the 2D and 3D images are plotted in μm , while the z-axis units in the 3D images are currently unspecified as they are specific to the user (arbitrary units, counts, etc.).

The process of generating the map images begins in section 26.

Before generating each map, an array of the necessary values is created from the complete results array (e.g. {x, y, G peak area}). The values from any fits that returned an error string instead of an integer, or that returned a negative value, are then removed from the array.

2D and 3D images of the intensity ratio 2D/G are created and exported before removing all areas from the complete results array for which the ratio is indicative of multilayer graphene (section 27). All of the following images will now only represent areas of single layer graphene..

Each 2D map is exported four times with different intensity scales. Once with the maximum and minimum limits of the intensity axis set by the maximum and minimum values contained in the array, and three more times with the upper limit reduced to 1/2, 1/4, and 1/10 of the maximum value. This is useful when dealing with surface-enhanced Raman spectroscopy as it makes the topology of the lower intensity areas more visible. A single, strongly-enhanced, hotspot can often completely dwarf the rest of the map, masking other areas of lesser, but still significant, enhancement.

Histograms of the distribution of G peak area values are generated in section 32 (func. 32.2). This allows the user to compute the average value, the distribution and standard deviation of values, and to precisely identify enhanced values. The histograms are fit with a Gaussian distribution, a gamma distribution and a log-Gaussian (log-normal) distribution. The user can then view the histograms and select the histogram plot with the highest χ^2 value as the best fit.

Mathematica has a very large number of mathematical distributions which can be easily incorporated. Simply search for "distribution" in the help menu for a comprehensive list.

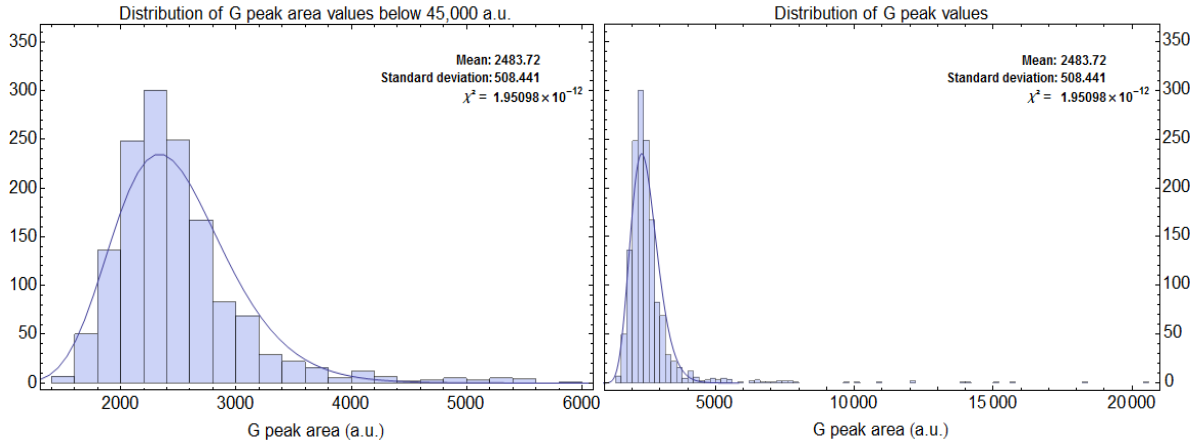


Fig. 9: (Left) A histogram of the data used to calculate the average (*distdatamax*=6000), fitted with a log-normal distribution. (Right) A histogram of the complete data set, including enhanced areas. For this data set the log-normal distribution fit the data best (highest χ^2 value) so it was selected as the final histogram and its values for the mean and standard deviation were used as results.

The distributions of the G peak area are only fitted to values up to a user-defined cut-off point (*distdatamax*), above which we do not accept values as contributing to the average. This is necessary in the presence of enhanced areas which would falsely influence the average. If enhancement is not present in the samples, simply remove this section or set the variable *distdatamax* to a value greater or equal to the highest G peak area observed in the map.

4.6.1 Complete list of images generated.

1. **map; I(2D G) mapname:** 2D plot of the ratio of the 2D/G peak amplitudes, z-axis scale: minimum value → maximum value. The intensity is interpolated across each data point. (sect. 26.5)
2. **map; I(2D G) 2 mapname:** 2D/G peak amplitudes, plotted in 2D, interpolated, z-axis scale: min. → max./2. (sect. 26.6)
3. **map; I(2D G) 4 mapname:** 2D/G peak amplitudes, plotted in 2D, interpolated, z-axis scale: min. → max./4. (sect. 26.7)
4. **map; I(2D G) 10 mapname:** 2D/G peak amplitudes, plotted in 2D, interpolated, z-axis scale: min. → max./10. (sect. 26.8)
5. **3D map; I(2D G) mapname:** 3D plot of the ratio of the 2D/G peak amplitudes, interpolated. (sect. 26.9)

6. **map; A(G) mapname:** Area of the G peak, plotted in 2D, interpolated, z-axis scale: minimum value → maximum value, multilayer areas removed. (sect. 28)
7. **map; A(G) 2 mapname:** Area of the G peak, plotted in 2D, interpolated, z-axis scale: min. → max./2, multilayer areas removed. (sect. 28)
8. **map; A(G) 4 mapname:** Area of the G peak, plotted in 2D, interpolated, z-axis scale: min. → max./4, multilayer areas removed. (sect. 28)
9. **map; A(G) 10 mapname:** Area of the G peak, plotted in 2D, interpolated, z-axis scale: min. → max./10, multilayer areas removed, multilayer areas removed. (sect. 28)
10. **3D map; A(G) mapname:** Area of the G peak, plotted in 3D, interpolated, multilayer areas removed. (sect. 28)
11. **3D map; A(G); square mapname:** Area of the G peak, plotted in 3D, multilayer areas removed. The intensity is presented in histogram blocks for each measurement. This is really only included to show the user that other plot options are available. (sect. 28.1)
12. **map; A(D) mapname:** Area of the D peak, plotted in 2D, interpolated, z-axis scale: minimum value → maximum value, multilayer areas removed. (sect. 29)
13. **map; A(D) 2 mapname:** Area of the D peak, 2D, z-axis scale: min. → max./2, multilayer areas removed. (sect. 29)
14. **map; A(D) 4 mapname:** Area of the D peak, 2D, z-axis scale: min. → max./4, multilayer areas removed. (sect. 29)
15. **map; A(D) 10 mapname:** Area of the D peak, 2D, z-axis scale: min. → max./10, multilayer areas removed. (sect. 29)
16. **3D map; A(D) mapname:** Area of the D peak, plotted in 3D, interpolated, multilayer areas removed. (sect. 29)
17. **map; A(2D) mapname:** Area of the 2D peak, plotted in 2D, interpolated, z-axis scale: minimum value → maximum value, multilayer areas removed. (sect. 30)
18. **map; A(2D) 2 mapname:** Area of the 2D peak, plotted in 2D, z-axis scale: min. → max./2, multilayer areas removed. (sect. 30)
19. **map; A(2D) 4 mapname:** Area of the 2D peak, plotted in 2D, z-axis scale: min. → max./4, multilayer areas removed. (sect. 30)
20. **map; A(2D) 10 mapname:** Area of the 2D peak, plotted in 2D, z-axis scale: min. → max./10, multilayer areas removed. (sect. 30)
21. **3D map; A(2D) mapname:** Area of the 2D peak, plotted in 3D, interpolated, multilayer areas removed. (sect. 30)

22. **map; strained A(2D) mapname:** Area of the strained 2D peak, plotted in 2D, interpolated, z-axis scale: minimum value → maximum value. (sect. 31)
23. **map; strained A(2D) 2 mapname:** Area of the strained 2D peak, plotted in 2D, z-axis scale: min. → max./2, multilayer areas removed. (sect. 31)
24. **map; strained A(2D) 4 mapname:** Area of the strained 2D peak, plotted in 2D, z-axis scale: min. → max./4, multilayer areas removed. (sect. 31)
25. **map; strained A(2D) 10 mapname:** Area of the strained 2D peak, plotted in 2D, z-axis scale: min. → max./10, multilayer areas removed. (sect. 31)
26. **3D map; strained A(2D) mapname:** Area of the strained 2D peak, plotted in 3D, interpolated, multilayer areas removed. (sect. 31)

27. **G peak area, average values histogram; Gaussian mapname:** A histogram of the data which was used to calculate the distributions, overlaid with the Gaussian distribution. The mean value, standard deviation and χ^2 value are shown in the top right corner. (sect. 32.2.1)
28. **G peak area, histogram; Gaussian mapname:** A histogram of the complete dataset with the Gaussian distribution. (sect. 32.2.2)
29. **G peak area, logarithmic histogram; Gaussian mapname:** A histogram of the complete dataset and Gaussian distribution, with a logarithmic scale on the x-axis. (sect. 32.2.3)

30. **G peak area, average values histogram; Gamma mapname:** (sect. 32.3)
31. **G peak area, histogram; Gamma mapname:** (sect. 32.3)
32. **G peak area, logarithmic histogram; Gamma mapname:** (sect. 32.3)

33. **G peak area, average values histogram; LogGaussian mapname:** (sect. 32.4)
34. **G peak area, histogram; LogGaussian mapname:** (sect. 32.4)
35. **G peak area, logarithmic histogram; LogGaussian mapname:** (sect. 32.4)

The following are additional images showing enhancement values which can be generated with the *map, histogram plotting programme* only:

36. **Enhancement map; A(G) mapname**
37. **Enhancement map; A(G) 2 mapname**
38. **Enhancement map; A(G) 4 mapname**
39. **Enhancement map; A(G) 10 mapname**

4 Data Analysis

40. 3D Enhancement map; A(G); square *mapname*
41. 3D Enhancement map; A(G) *mapname*

42. G peak enhancement, average values histogram; Gamma *mapname*
43. G peak enhancement, average values histogram; Gaussian *mapname*
44. G peak enhancement, average values histogram; LogGaussian *mapname*

45. G peak enhancement, histogram; Gamma *mapname*
46. G peak enhancement, histogram; Gaussian *mapname*
47. G peak enhancement, histogram; LogGaussian *mapname*

48. G peak enhancement, logarithmic histogram; Gamma *mapname*
49. G peak enhancement, logarithmic histogram; Gaussian *mapname*
50. G peak enhancement, logarithmic histogram; LogGaussian *mapname*

Additional Programmes

5.1 Map, histogram plotting programme

This programme contains the map fitting section of the main programme. It allows the user to generate maps and histograms from the fit results without having to repeat the, often time-consuming, plot fitting computation.

This is invaluable as one often finds oneself needing to edit axes labels, font size, etc. on images before presenting them and the variables *distdatamax* and *bin* can often be hard estimate before seeing the results.

In this programme we also create a second set of histograms which are normalized with respect to a reference sample. In the case of SERS, this allows the user to determine the enhancement factor of a sample with respect to an unenhanced reference sample. This can also be used to normalize the sample with respect to the average peak area, allowing the user to determine the distribution of values.

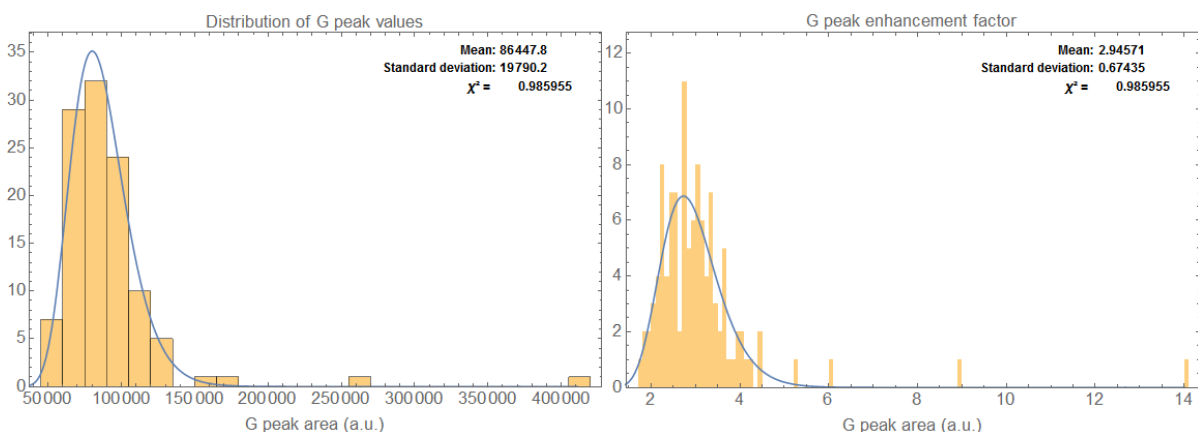


Fig. 10: (Left) A histogram of G peak area values from a sample of graphene on nanostructured copper. (Right) The same histogram, with different bin sizes, after normalization with respect to a reference sample of graphene on a single-crystal, polished, Cu[111] substrate. A general enhancement of ~ 3 times the unenhanced Raman signal occurs across the sample, as well as a 'hotspot' with an enhancement factor of ~ 14 .

5.2 Normalization programme

A programme for multiplying the intensity values of the spectra by a constant value. This is used to normalize data from different laser wavelengths which may have different intensities, or measurements with different acquisition times.

Each file in the data set is imported, the y-values are edited, and the new file is exported to a folder named *mapname*;Normalized in the parent folder of the original data set.

5.3 Single plot checker

A programme for checking fit parameters, etc. on individual spectra. This is useful when editing the fit parameters for a change of wavelength or an unusual background, or to improve the over-all peak fits.

All relevant parameters are returned in the Mathematica window as the programme runs, as well as spectra of the background and each peak with their respective plot functions.

This is also useful when editing the colour-scheme, font-size, etc. of the spectra.

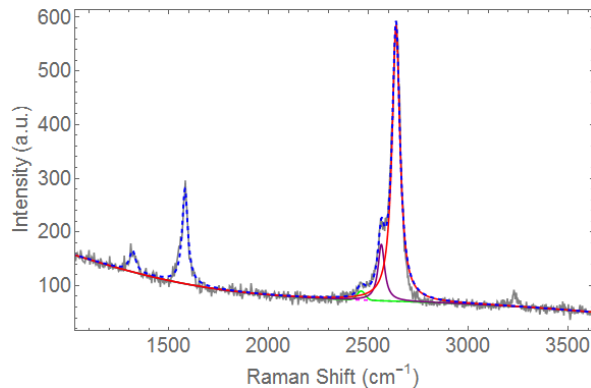


Fig. 11: A typical spectrum as they are currently formatted. Each spectrum is individually plotted and exported.

5.4 PolynomialFit.m

This is an external Mathematica function which has been replaced in newer versions of Mathematica. It returns an error message which states that it is no longer supported in current version of Mathematica. This can be ignored, however.

This function allows us to choose the degree of the polynomial we wish to use, allowing the user to ensure that the background fit is accurate. It returns a polynomial function with respect to x which is in the correct format for use with the peak fitting functions.

Bibliography

- [1] J. Hedberg, [Online]. Available:
<http://www.jameshedberg.com/img/samples/graphene-sheet-atoms.jpg>. [Accessed: 13-Jun-2015].
- [2] D. L. Jeanmaire and R. P. Van Duyne, “Surface raman spectroelectrochemistry: Part I. Heterocyclic, aromatic, and aliphatic amines adsorbed on the anodized silver electrode,” *J. Electroanal. Chem. Interfacial Electrochem.*, vol. 84, no. 1, pp. 1–20, Nov. 1977.
- [3] M. Moskovits, “Surface roughness and the enhanced intensity of Raman scattering by molecules adsorbed on metals,” *J. Chem. Phys.*, vol. 69, no. 9, p. 4159, 1978.
- [4] M. G. Albrecht and J. A. Creighton, “Anomalously intense Raman spectra of pyridine at a silver electrode,” *J. Am. Chem. Soc.*, vol. 99, no. 15, pp. 5215–5217, 1977.
- [5] D. Yoon, Y.-W. Son, and H. Cheong, “Negative Thermal Expansion Coefficient of Graphene Measured by Raman Spectroscopy,” *Nano Lett.*, vol. 11, no. 8, pp. 3227–3231, Aug. 2011.
- [6] K. S. Novoselov, A. K. Geim, S. V. Morozov, D. Jiang, M. I. Katsnelson, I. V. Grigorieva, S. V. Dubonos, and A. A. Firsov, “Two-dimensional gas of massless Dirac fermions in graphene,” *Nature*, vol. 438, no. 7065, pp. 197–200, Nov. 2005.
- [7] Y. Zhang, Y.-W. Tan, H. L. Stormer, and P. Kim, “Experimental observation of the quantum Hall effect and Berry’s phase in graphene,” *Nature*, vol. 438, no. 7065, pp. 201–204, Nov. 2005.
- [8] W. Xu, J. Xiao, Y. Chen, Y. Chen, X. Ling, and J. Zhang, “Graphene-Veiled Gold Substrate for Surface-Enhanced Raman Spectroscopy,” *Adv. Mater.*, vol. 25, no. 6, pp. 928–933, Feb. 2013.
- [9] W. Xu, N. Mao, and J. Zhang, “Graphene: A Platform for Surface-Enhanced Raman Spectroscopy,” *Small*, vol. 9, no. 8, pp. 1206–1224, Apr. 2013.
- [10] D. Prasai, J. C. Tuberquia, R. R. Harl, G. K. Jennings, and K. I. Bolotin, “Graphene: Corrosion-Inhibiting Coating,” *ACS Nano*, vol. 6, no. 2, pp. 1102–1108, Feb. 2012.
- [11] M. Topsakal, H. Şahin, and S. Ciraci, “Graphene coatings: An efficient protection from oxidation,” *Phys. Rev. B*, vol. 85, no. 15, Apr. 2012.

- [12] M. Schriver, W. Regan, W. J. Gannett, A. M. Zaniewski, M. F. Crommie, and A. Zettl, “Graphene as a Long-Term Metal Oxidation Barrier: Worse Than Nothing,” *ACS Nano*, vol. 7, no. 7, pp. 5763–5768, Jul. 2013.
- [13] S. Heeg, A. Oikonomou, R. F. Garcia, S. A. Maier, A. Vijayaraghavan, and S. Reich, “Strained graphene as a local probe for plasmon-enhanced Raman scattering by gold nanostructures: Strained graphene as a local probe for plasmon-enhanced Raman scattering by gold nanostructures,” *Phys. Status Solidi RRL - Rapid Res. Lett.*, vol. 7, no. 12, pp. 1067–1070, Dec. 2013.
- [14] S. Reich and C. Thomsen, “Raman spectroscopy of graphite,” *Philos. Trans. R. Soc. Math. Phys. Eng. Sci.*, vol. 362, no. 1824, pp. 2271–2288, Nov. 2004.
- [15] C. S. S. R. Kumar, Ed., *Raman Spectroscopy for Nanomaterials Characterization*. Berlin, Heidelberg: Springer Berlin Heidelberg, 2012.
- [16] C. Thomsen and S. Reich, “Double resonant Raman scattering in graphite,” *Phys. Rev. Lett.*, vol. 85, no. 24, p. 5214, 2000.
- [17] A. C. Ferrari and D. M. Basko, “Raman spectroscopy as a versatile tool for studying the properties of graphene,” *Nat. Nanotechnol.*, vol. 8, no. 4, pp. 235–246, Apr. 2013.
- [18] R. J. Nemanich and S. A. Solin, “First-and second-order Raman scattering from finite-size crystals of graphite,” *Phys. Rev. B*, vol. 20, no. 2, p. 392, 1979.
- [19] D. Yoon, H. Moon, H. Cheong, J. S. Choi, J. A. Choi, and B. H. Park, “Variations in the Raman Spectrum as a Function of the Number of Graphene Layers,” *J Korean Phys Soc*, vol. 55, no. 3, pp. 1299–1303, 2009.
- [20] M. S. Dresselhaus, A. Jorio, M. Hofmann, G. Dresselhaus, and R. Saito, “Perspectives on Carbon Nanotubes and Graphene Raman Spectroscopy,” *Nano Lett.*, vol. 10, no. 3, pp. 751–758, Mar. 2010.
- [21] L. M. Malard, J. Nilsson, D. C. Elias, J. C. Brant, F. Plentz, E. S. Alves, A. H. Castro Neto, and M. A. Pimenta, “Probing the electronic structure of bilayer graphene by Raman scattering,” *Phys. Rev. B*, vol. 76, no. 20, Nov. 2007.
- [22] “Multilayer CVD graphene,” *Portland State University, The Lab of Nanoelectronics*. [Online]. Available: <http://www.pdx.edu/nanoelectronics/graphene>. [Accessed: 08-Jun-2015].
- [23] O. Frank, M. Mohr, J. Maultzsch, C. Thomsen, I. Riaz, R. Jalil, K. S. Novoselov, G. Tsoukleri, J. Parthenios, K. Papagelis, L. Kavan, and C. Gallois, “Raman 2D-Band Splitting in Graphene: Theory and Experiment,” *ACS Nano*, vol. 5, no. 3, pp. 2231–2239, Mar. 2011.